

# Copper microwires spun from the melt

G. MANFRÈ, G. SERVI, C. RUFFINO

Montedison S.p.A., Istituto Ricerche "G. Donegani", Novara, Italy

To obtain metal fibres of diameter less than 50  $\mu\text{m}$ , the Taylor method has been developed for copper microwires to exploit their electrical and electronic applications. We have tested the dependence of continuity, grain size, texture and mechanical properties on the process parameters as well as drawing ratio and quenching time. Grain arrangement and the elastic-plastic behaviour of the fibres are discussed.

## 1. Introduction

The demand for cheap production of metal fibres is rapidly increasing both in the field of composite materials and for electronic and electrical applications. The cold drawn process is widely used, but the cost of fibres produced by this method increases as fibre diameter decreases. This limits their commercial applications. To overcome this difficulty new production technologies have been developed in the last decade such as melt extrusion [1], melt drug [2], solidification against a cooled surface [3] and, more recently, a new development of the Taylor process [4, 5] and the Wollastone technology [6].

Of these methods the authors [7] and Butler *et al* [8] have shown that so far the Taylor process is more suitable for obtaining fibres less than 100  $\mu\text{m}$ .

In the present paper we deal with copper fibres less than 50  $\mu\text{m}$  diameter obtained by a technology [4, 5] which is a development of the elementary Taylor process. The aim of this paper is to show some relationship between process parameters and mechanical properties. A morphological description and structural parameters, such as grain size and texture of the microwires will be given.

## 2. Experimental part

### 2.1. Microwires spinning apparatus

Equipment to spin microwires has been set up following the initial Taylor idea. The apparatus consists of a device causing the downward motion, at a constant rate, of a glass tube containing a rod of copper. A special furnace,

heated by a resistor or induction coil, softens the entering glass tube at a temperature above the melting point of copper forming a continuous stream drawn by a rotating drum which collects the microwire at a constant speed. Fig. 1 shows the sketch of the apparatus equipped with a

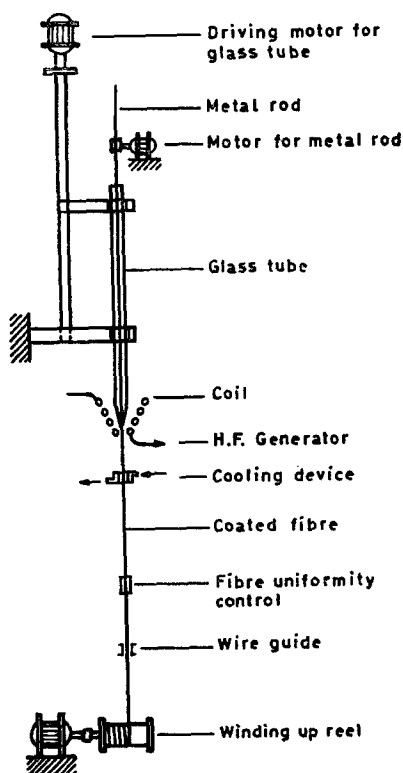


Figure 1 Apparatus for spinning glass-coated microwires (schematic).

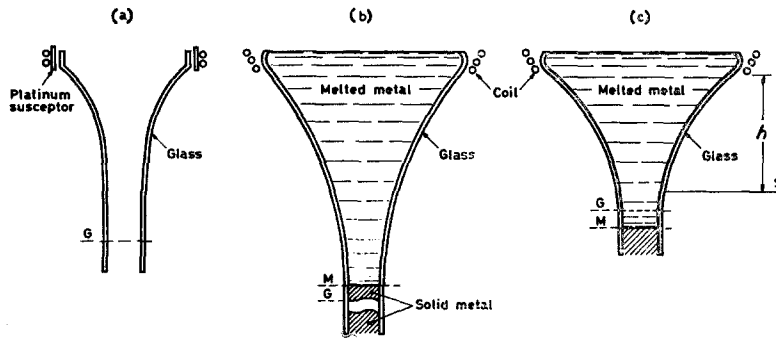


Figure 2 Drawing zone profiles of: (a) glass capillary; (b) glass coated microwire cooling with air; (c) as (b) cooling with a liquid. G: glass solidification point, M: metal crystallization point, *h*: distance between furnace and cooling device.

device cooling the drawing zone at a certain distance below the furnace. An automatic control of heating temperature as well as of glass tube and drawing speeds was necessary to stabilize the process and to obtain continuous fibres.

As far as continuity is concerned cooling of the drawing zone was found necessary to get continuous microwires. The reason for this seems that the cooling system shortens the drawing zone so that solidification of the metal will occur once the stretching of the glass has been accomplished. The main parameters of the process are: drawing ratio, temperature and its gradient, drawing zone cooling position, glass viscosity and its variation with temperature and the thermal expansion coefficient of both metal and glass.

2.2. The melt spinning process parameters

The values of process parameters in spinning glass covered microwires cooling the drawing

zone with air, SR, or a liquid, CR, are shown in Table I. There  $\Phi_{Cu}$  is the fibre diameter,  $V_t$  is the speed of the glass tube,  $V_d$  is the collecting drum speed, *R* is the drawing ratio between the copper rod and metallic fibre diameter, and *h* is the distance between the bottom of the furnace and upper surface of the cooling device (Fig. 2).

The temperature in the heating device rises up to 1300°C and at this temperature swelling of the glass and melting of the metal occur. The temperature then decreases to the softening point of the glass in the drawing zone, which varies in length as shown in Fig. 2. The end of the drawing zone is considered the point at which the total diameter of the microwire begins to be constant. Generally speaking, crystallization of the copper may occur before or after achieving the final diameter.

On the other hand, if the metal crystallizes before the glass solidification point, the metal core breaks in the subsequent drawing of glass

TABLE I Typical process parameters data in spinning from melt SR and CR copper microwires of 10 to 40 μm in diameter

$\Phi_{Cu}$ (μm)	$\Phi_{tot}^*$ (μm)	Type	$V_t$ (mm min <sup>-1</sup> )	$V_d$ (round min <sup>-1</sup> )	<i>R</i>	<i>h</i> (mm)
10	20	SR	12	240	550	—
20	50	SR	12	120	275	—
30	70	SR	12	55	183	—
40	90	SR	12	30	137.5	—
10	20	CR	12	240	550	4
20	48	CR	12	125	275	4
30	60	CR	12	50	183	4
40	95	CR	12	35	137.5	4

\* $\Phi_{tot}$  is total diameter, metal plus glass, of the fibre.

before final diameter is achieved, so giving an interrupted metal microwire.

### 2.3. Testing procedures

Samples obtained in the spinning conditions shown in Table I, were observed by X-rays and the optical and scanning electron microscope. The fibres were vertically and horizontally embedded in Araldite and polished with alumina powders up to  $0.05\ \mu\text{m}$  to obtain a specular copper surface. Chemical etching with  $\text{HNO}_3\text{-H}_3\text{PO}_4\text{-CH}_3\text{COOH}$  (40-50-10%) revealed a grain structure whose size was measured on optical micrographs of longitudinal sections of the microwires. Hejn's procedure, which seems the best method considering also sample geometry, was used on five different fields containing 50 grains each.

Work on morphological characteristics of the microwires and grain arrangement was performed by SEM.

Texture was determined by X-ray diffraction with a flat camera geometry on a rotating sample and with a double circle diffractometer using  $\text{CuK}\alpha$  radiation.

An Instron TS table dynamometer was used to test the mechanical properties of the fibres, after dissolving off the glass using an HF solution, at a crosshead speed of  $0.5\ \text{cm min}^{-1}$ . The specimens had a gauge length of 5 cm or 20 cm. The values shown are the average of twenty tests for each sample.

### 3. Results

In Fig. 3, viscosity versus temperature is shown on the semi-logarithmic scale, for the most common glasses and fcc metals. In spinning copper the glass must have a viscosity almost  $10^6$  P at the crystallization temperature of the metal.

The best results in spinning copper are obtained using "Supremax" glass with a thermal expansion coefficient of  $4.1 \times 10^{-6}$  parts  $^\circ\text{C}^{-1}$  against  $17 \times 10^{-6}$  parts  $^\circ\text{C}^{-1}$  of the metal, providing that the final ratio between glass thickness and copper radius is  $\Delta_g/\Delta_m = 1$  to 1.4. The microwires obtained by cooling the drawing zone with a liquid are continuous for several hundred metres; in particular, from 100 to  $30\ \mu\text{m}$  diameter there are 1 to 3 interruptions over several thousand metres and 1 to 3 interruptions over one hundred metres, when the diameter is about  $10\ \mu\text{m}$ . Fibres obtained without cooling have almost one interruption per metre.

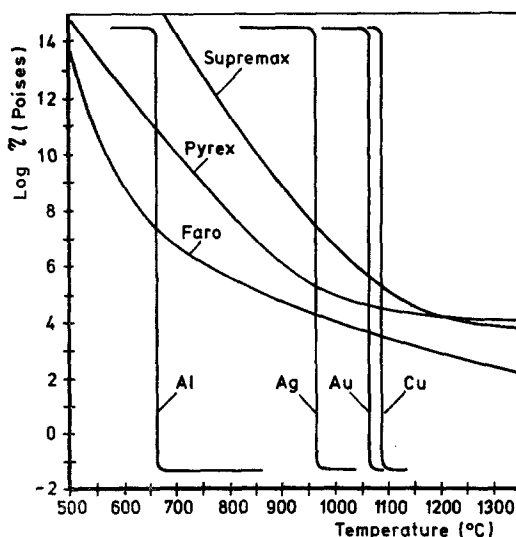


Figure 3 Viscosity versus temperature diagram for the most common glasses and fcc metals.

Continuous microwires on longitudinal and transversal sections appear uniform without any bubbles, voids or cracks in the glass, even at very low diameters. The higher shrinkage of the metal produces an overriding compressive force which relieves the tension of the glass allowing it to be subjected to very small bending radii.

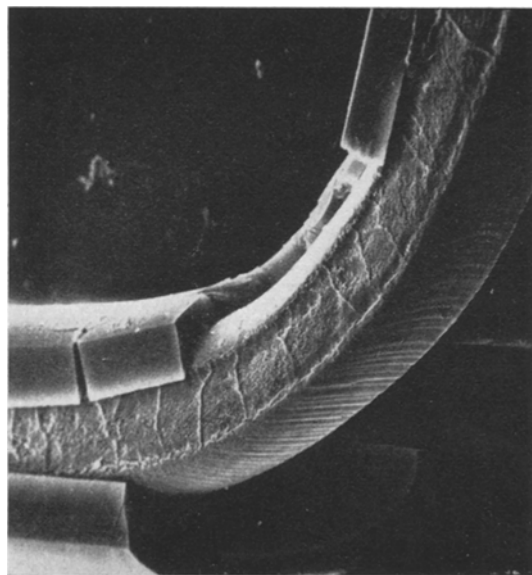


Figure 4 SEM micrograph of a glass-coated microwire ( $\Phi_{\text{Cu}} = 30\ \mu\text{m}$ ) ( $\times 815$ ).

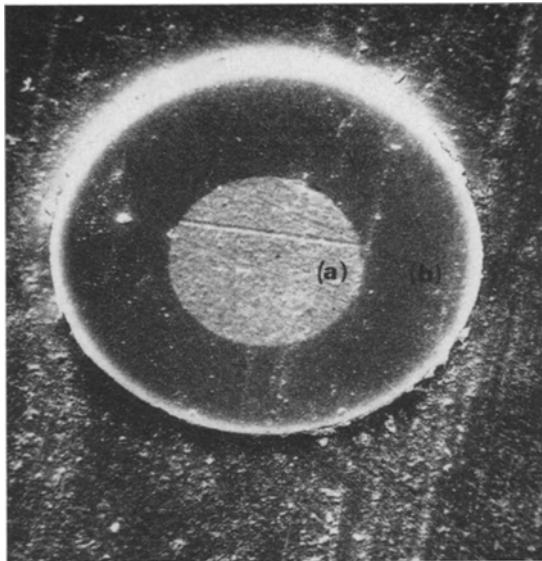


Figure 5 SEM transversal micrograph of a copper microwire ( $\Phi_{Cu} = 30 \mu\text{m}$ ,  $\Phi_{tot} = 60 \mu\text{m}$ ). (a) metal core; (b) glass coating ( $\times 783$ ).

A general view of a copper fibre is presented in Fig. 4. It shows a microwire lapped, etched and bent before scanning electron microscope observation. The inside glass surface is very smooth, no defects are visible, the same is true of metal interface.

Particular attention was devoted to the glass metal interface which is very important for the properties of the "composite" and for the

mechanical characteristics of the copper when the glass is dissolved away. Several transverse sections of microwires vertically embedded were observed by SEM and on carbon replica by TEM.

As is shown in Figs. 5 and 6, the different techniques give similar results, thus glass and metal are in close contact. Experiments [9] carried out in a thermal differential analysis apparatus with copper and glass powders show that metal does not wet the glass, but in some case the former can be oxidized at the interface and copper oxide may diffuse in the glass. In the microwires this phenomenon is not present, no chemical reaction takes place at the spinning stage so the metal glass adhesion is to be ascribed to the differential thermal expansion as mentioned above.

Texture axis determination of microwires is difficult. The typical X-ray diffraction pattern of Fig. 7a was obtained with a flat camera on a rotating sample. It consists of four  $\{111\}$  and two  $\{200\}$  spots for each quadrant whose azimuthal angles  $\delta$  do not exactly correspond to any interplanar angle.

The spot geometry and the grain arrangement shown in Fig. 8 suggest that this pattern arises from a polycrystal whose grains, built up one upon another like bricks, simulate a single crystal behaviour in the respect of X-ray diffraction. So it is possible to define a reciprocal lattice for the polycrystalline fibre with the  $[001]$  axis forming an angle  $\delta$  with the physical axis  $z$  of the fibre. In such a way the spots of Fig.

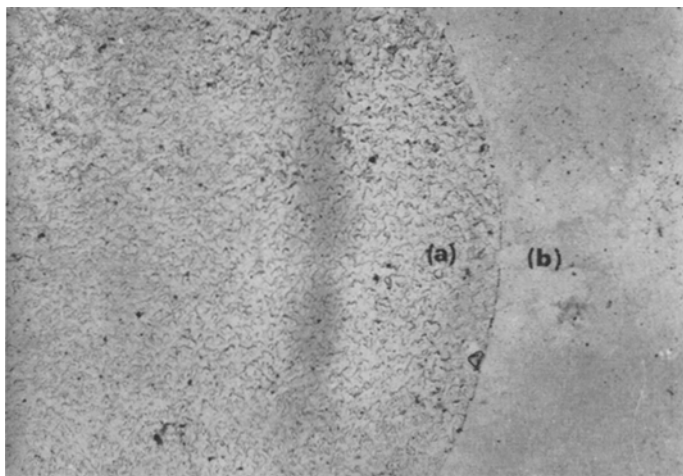


Figure 6 TEM transversal micrograph of a detail of a copper microwire ( $\Phi_{Cu} = 30 \mu\text{m}$ ,  $\Phi_{tot} = 60 \mu\text{m}$ ). Carbon replica ( $\times 3325$ ).

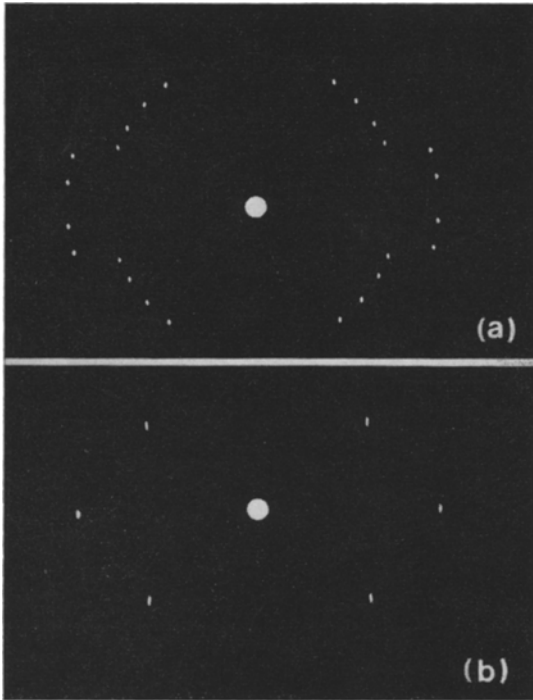


Figure 7 Typical transmission texture patterns of micro-wires spun from melt. (a) X-ray diffraction diagram with fibre perpendicular to the beam; (b) X-ray diffraction diagram after fibre re-orientation (on the Stoe two circle diffractometer). Texture axis is [100].

7a may be generated by the intersection of the reciprocal lattice planes with the Ewald sphere. A Stoe two circle diffractometer has been used to verify the angular position of the spots, to orient the sample and to put [001] axis of the cell parallel to the rotation axis of the sample holder. The sample so oriented gives the single crystal-like diagrams of Fig. 7b and we were able to measure experimentally the angle between physical axis  $z$  and texture axis of the fibre. Results were confirmed by simple calculations on the reciprocal lattice cylindrical co-ordinates of the spots of Fig. 7a.

The texture as a function of fibre diameter is shown in Table II. All micro-wires present a single texture axis with an almost perfectly developed fibre structure. The angular misorientation between  $z$  and texture axis is exactly the same for all grains in the micro-wires. That is all crystals have [100] lattice direction at a well defined angle  $\delta$  with  $z$  axis and only in that position may the texture axis be found. It is worth noting that misorientation increases with fibre diameter, in accordance with the decrease

of the drawing ratio  $R$ , and that values are less for CR than for SR fibres. The situation is different for the cold drawn copper microwires which present a statistical deviation of the crystals about the fibre axis. Moreover these fibres have shown a double texture [100] + [111] as reported in the literature [10-12] when the deformation is below 96% reduction in diameter.

TABLE II Fibre texture and misorientation between texture and  $z$  axis for SR and CR copper microwires spun from melt

Diameter ( $\mu\text{m}$ )	Type	Texture axis	Misorientation between $z$ and texture axis
10	SR	[100]	3° 50'
20	SR	[100]	8° 10'
30	SR	[100]	15° 21'
40	SR	[100]	14° 08'
10	CR	[100]	4° 04'
20	CR	[100]	2° 30'
30	CR	[100]	14° 07'
40	CR	[100]	11° 50'

Grain structure is another important characteristic of these melt spun microwires. The particular arrangement of Fig. 8 shows grain boundaries nearly normal to the wire axis and a well defined stacking holding for long tracts. Grains appear well formed, sometimes the width of half the fibre section but only a few microns long. Grain size and tensile properties are shown in Table III.

It should be noted that, in the case of CR fibres, the influence of the drawing ratio on grain size seems greater than that of SR fibres. This depends mainly on the quenching time of the drawing zone or, in other words, on the heat transfer coefficient from the forming fibre surface [13].

Concerning mechanical characteristics, the melt spun microwires can be considered an elastic-plastic material, as shown in Fig. 9 by the stress-strain curve. The plot shows a very sharp transition between the elastic and plastic parts. The linear elastic part presents a very sharp yield point at which plastic deformation starts at nearly constant stress. Table III shows that the ultimate tensile strength  $\sigma_{UTS}$  differs very little from the  $\sigma_{0.2\%}$  (stress at 0.2% elongation). This feature shows the absence of a locking mechanism of dislocations generated under the applied stress, as expected in fcc

TABLE III Typical  $\sigma_{0.2}$ %,  $\sigma_{UTS}$ , total elongation% data at different diameters and grain sizes for CR and SR copper microwires spun from melt

Diameter ( $\mu\text{m}$ )	Type	Grain size $d(\text{mm})$	$\sigma_{0.2}$ % (kgf mm <sup>-2</sup> )	$\sigma_{UTS}$ (kgf mm <sup>-2</sup> )	Total elongation (%)
10	SR	3.20	7.50	8.6	9.80
20	SR	4.83	5.80	6.9	11.20
30	SR	4.95	7.00	7.5	13.25
40	SR	5.24	6.50	7.0	15.30
10	CR	1.15	17.00	18.0	8.15
20	CR	1.82	9.20	10.0	10.20
30	CR	2.70	8.00	9.2	12.70
34	CR	4.20	—	—	—
40	CR	7.55	5.20	5.8	13.10

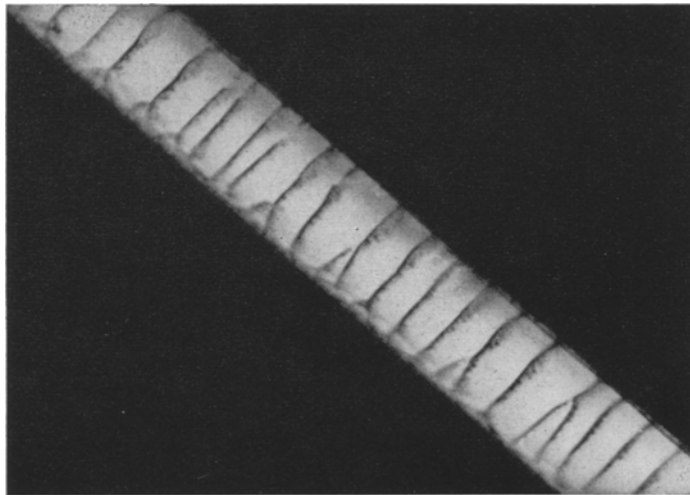


Figure 8 Transversal optical micrograph showing grain arrangement in a copper microwire ( $\Phi_{CV} = 40 \mu\text{m}$ ) Grain boundaries are almost perpendicular to the  $z$  axis of the microwire ( $\times 600$ ).

metals of ordinary purity [14]. In accordance with this situation the total percentage elongation is quite high and increases as  $\sigma_{UTS}$  decreases. Flow stress appears independent of grain size for SR fibres [14] while no simple relation seems to hold for CR fibres.

#### 4. Discussion

The main structural characteristics of these copper melt spun microwires are the size and arrangement of grains. The size is mainly a function of the cooling method of the drawing zone and of the drawing ratio  $R$ .

The arrangement of grains is such that the boundaries are nearly perpendicular to the fibre axis. This is thought to be owing to the compressive force of the glass on the copper.

The glass, solidifying before crystallization of the metal, shrinks the molten metal affecting the stacking and the configuration of grains.

The stacking is such that the grains are built up like bricks one upon another with [100] crystallographic axis nearly parallel to the fibre axis. This structure has been confirmed by texture patterns and by SEM micrographs. Cold drawn microwires differ in texture, grain size and arrangement. Their texture is [111] + [100], as reported in the literature and verified by authors, and except for these directions the grains are randomly arranged and their size is considerably smaller (1 to 3  $\mu\text{m}$ ). These differences in structural configuration and the different hardening lead to different mechanical properties. In particular  $\sigma_{0.2}$  and  $\sigma_{UTS}$  are

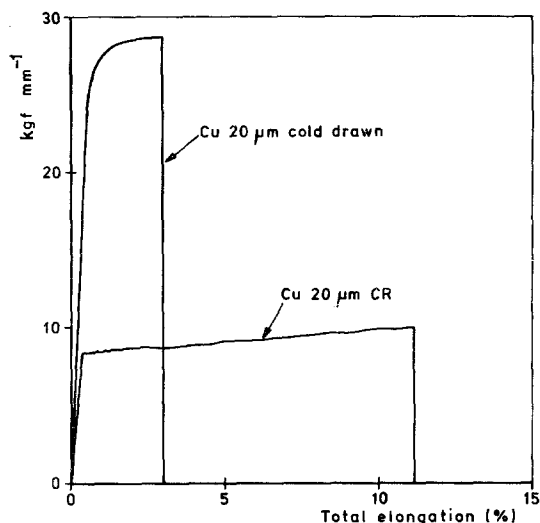


Figure 9 Stress versus total percentage elongation diagram for cold drawn and melt spun microwires ( $\phi_{\text{Cu}} = 20 \mu\text{m}$ ).

higher than those of melt spun microwires and the former value is considerably lower than the latter. The total percentage elongation is however much lower (Fig. 9). At the actual state of the work the most important relationships gained between spin variables and fibre structure is the dependence of grain size and texture misorientation on drawing ratio and quenching time.

This result and the perfect knowledge of the drawing zone profile will enable finer grained metallic fibres to be obtained by the melt spun method. The interpretation of the large plastic deformation of the fibres at a nearly constant stress and the grain size sensitivity of flow stress for CR microwires require further research.

The morphological aspects of the fibres lead to the conclusion that continuity depends on both glass characteristics and cooling method of the drawing zone.

## 5. Conclusion

Taylor's method has been developed to obtain

continuous copper microwires ranging between 10–50  $\mu\text{m}$  in diameter. Continuity, grain size and texture depend on spinning variables like drawing ratio and quenching time. The particular grain arrangement seems to be due to the compressive force exerted by the glass on the molten metal just before crystallization.

The approach to establishing a relationship between structure and mechanical properties lead us to think that, so far, by this method only microwires showing an elastic-work-hardening behaviour can be obtained. However, the microwires present properties suitable for electrical and electronic applications as well as reinforcements in composites.

## Acknowledgement

The authors wish to thank Dr A. Mula and Mr M. Solari, of Montedison-Bollate Research Centre, for scanning electron micrographs.

## References

1. C. E. ANAGNOSTOPOULOS, *Rubber J.* **152** (1970) 23.
2. D. L. KING, *Metals* **2** (1967) 33.
3. US Patent 2.825.108 (R. B. Pond) (1958).
4. US Patent 3.362.803 (Secretary of Defence, Fed. Rep. Germany) (1968).
5. G. MANFRÈ and D. VIANELLO, Italian Patent 930.409 (Montedison S.p.A.) (1972).
6. US Patent 3.505.039 (Brunswick Co.) (1970).
7. G. MANFRÈ, Comptes rendues assemblée générale société chimique de Belgique, Section Systèmes Amorphes et Vitreux, Bruxelles, 15-16 March 1973.
8. I. G. BUTLER, W. KURTZ, J. GILLOT and B. LUX, *Fibre Sci. & Tech.* **5** (1972) 243.
9. F. GALANTE and G. MANFRÈ, *Ceramurgia* **3** (1) (1973).
10. E. SCHMID and G. WASSERMAN, *Z. Physik* **42** (1927) 779.
11. I. DILLAMORE and W. ROBERTS, *Met. Rev.* **10** (39) (1965) 271.
12. N. BROWN, *Transaction AIME* **221** (1961) 236.
13. G. MANFRÈ, *Verres Réfract.* **26** (2) (1972) 57.
14. R. ARMSTRONG, I. CODD, R. DOUTHWAITE and N. PETCH, *Phil. Mag.* **7** (1962) 45.

Received 23 May and accepted 27 June 1973.